Received: 19 June 2024 | Revised: 5 August 2024 | Accepted: 8 August 2024

DOI: 10.1002/jmor.21765

RESEARCH ARTICLE

JOURNAL OF morphology WILEY

Ultrastructure of the extraordinary pedal gland in *Asplanchna* aff. *herricki* (Rotifera: Monogononta)

Rick Hochberg[1] | Robert L. Wallace[2] | Elizabeth J. Walsh[3] | Thiago Q. Araújo[1]

[1]Department of Biology, University of Massachusetts Lowell, Lowell, Massachusetts, USA

[2]Department of Biology, Ripon College, Ripon, Wisconsin, USA

[3]Department of Biological Sciences, University of Texas at El Paso, El Paso, Texas, USA

Correspondence
Rick Hochberg, Department of Biological Sciences, University of Massachusetts Lowell, One Univ. Ave., Lowell, MA 01854, USA.
Email: rick_hochberg@uml.edu

Funding information
National Science Foundation, Grant/Award Numbers: DEB 2051684, DEB 2051704, DEB 2051710

Abstract

Rotifers possess complex morphologies despite their microscopic size and simple appearance. Part of this complexity is hidden in the structure of their organs, which may be cellular or syncytial. Surprisingly, organs that are cellular in one taxon can be syncytial in another. Pedal glands are widespread across Rotifera and function in substrate attachment and/or egg brooding. These glands are normally absent in *Asplanchna*, which lack feet and toes that function as outlets for pedal glandular secretions in other rotifers. Here, we describe the ultrastructure of a pedal gland that is singular and syncytial in *Asplanchna* aff. *herricki*, but is normally paired and cellular in all other rotifers. *Asplanchna* aff. *herricki* has a single large pedal gland that is active and secretory; it has a bipartite, binucleate, syncytial body and a cytosol filled with rough endoplasmic reticulum, Golgi, and several types of secretory vesicles. The most abundant vesicle type is large and contains a spherical electron-dense secretion that appears to be produced through homotypic fusion of condensing vesicles produced by the Golgi. The vesicles appear to undergo a phase transition from condensed to decondensed along their pathway toward the gland lumen. Decondensation changes the contents to a mucin-like matrix that is eventually exocytosed in a "kiss-and-run" fashion with the plasma membrane of the gland lumen. Exocytosed mucus enters the gland lumen and exits through an epithelial duct that is an extension of the syncytial integument. This results in mucus that extends from the rotifer as a long string as the animal swims through the water. The function of this mucus is unknown, but we speculate it may function in temporary attachment, prey capture, or floatation.

KEYWORDS
exocrine, mucus, secretion, zooplankton

1 | INTRODUCTION

The ancestral rotifer body plan is an open question. A recent study (Vasilikopoulos et al., 2024) using sequence-based phylogenomics and gene collinearity provides strong support for relationships among the four major lineages of Rotifera—Monogononta, Acanthocephala, Seisonidea, and Bdelloidea—but relationships within the largest clade, Monogononta, are poorly resolved (Sørensen & Giribet, 2006). Lack of phylogenetic resolution within this taxon (~1600 spp.) prevents plausible ancestral reconstructions that can be used to determine character evolution with respect to organ systems, behaviors, life histories, and ecologies (Hardy & Linder, 2005). This knowledge gap hinders understanding of the ancestral mode of reproduction in rotifers (e.g., biparental sex with full-size males or dwarf males, cyclical parthenogenesis with haploid males, etc.) and affiliated organ systems (e.g., paired or singular germaria and/or vitellaria, etc.), which may be correlated with habitat (e.g., marine, estuarine, freshwater) and lifestyle (e.g., benthic, meiobenthic, semiplanktonic, planktonic, sessile, colonial).

Rotifers are often portrayed as being mostly planktonic animals, and, in fact, much of the diversity in the largest lineage Monogononta does contain an abundance of planktonic species that tend to be more well-known than psammic species (Ejsmont-Karabin, 2023; Obertegger & Wallace, 2023; de Paggi et al., 2020). Many holoplanktonic rotifers are oviparous and brood their eggs until hatching (Gilbert, 1983, 1988; Sudzuki, 1955, 1957a, 1957b), while others may release eggs into the water where they sink to the bottom (Gilbert, 1983), or the females may temporarily descend to the benthos themselves or explore a substrate for oviposition (Gilbert, 1983). In general, psammic, benthic, and epiphytic species tend to oviposit on substrata (Gilbert, 1983; Walsh, 1989). Alternatively, most sessile taxa tend to retain their eggs closely opposed to their bodies (Davies et al., 2024). Some rotifers may, however, be considered functionally semiplanktonic because they can switch between a close association with surfaces and being completely planktonic during their lives, thereby exploiting both environments for feeding, mating, and oviposition (as noted above), and perhaps to escape predation. Species of the genus *Asplanchnopus* may be described as semiplanktonic: they regularly swim through littoral waters and generally only descend to a substratum to oviposit their eggs (Wurdak, 2017). In *Euchlanis dilatata* Ehrenberg, 1832, this behavior is generally preceded by some exploration of the substrate before attachment with their foot/toes and affiliated pedal glands before oviposition (Walsh, 1989).

Being exclusively ovoviviparous (Gilbert, 1983; Gilbert et al., 1989; but see Bentfeld, 1971 for potential viviparity), species of the holoplanktonic genus *Asplanchna* differ from most other rotifers (Gilbert, 1983, Gilbert et al., 1989); that is, descent to a substratum for oviposition is not part of their reproductive behaviors as they release functional juveniles directly into the water column. Moreover, the adult bodies appear well adapted for a strictly holoplanktonic lifestyle: transparency gives them effective camouflage against visual predators, their voluminous body cavities would seem to ease the energetics of floatation, and they have no foot or toes. *Asplanchna* is the sister taxon to the semiplanktonic *Asplanchnopus* according to the phylogeny of Walsh et al. (2005), which means their ancestor may well have had a semiplanktonic existence and at one time explored substrata for the purposes of oviposition.

One peculiar species of *Asplanchna*, *Asplanchna herricki* Guerne, 1888, was redescribed in 1893 by Wierzejski to possess toes and pedal glands. Little is known of its behavior and morphology beyond generic light microscopical observations, and there is no evidence that the glands engage in secretion. Some researchers have considered the glands to be vestigial and nonfunctional for these reasons (Koste, 1978; de Paggi, 2002). Yet, there is no evidence to suggest that the glands are vestigial. We recently encountered a morphotype of the species that does engage in active secretion, which allowed us to explore the ultrastructure and function of the glands and determine if they are similar to those of other rotifers.

2 | METHODS

Plankton samples were collected from Flint Pond in Massachusetts, USA (42°4′30.4″N, 71°25′32.9″W) with a 63-μm mesh net in summer 2023. Specimens of *Asplanchna* were removed and placed in a small bowl (3 mls) of ambient pond water and their behaviors were recorded with a Sony Handycam digital camera mounted on a Zeiss Stemi stereomicroscope. Drops of carbonated water were added to the bowls to anesthetize swimming rotifers for mounting on glass slides and photographing with a JENOPTIK GRYPHAX® AVIOR camera mounted on a Zeiss A1 compound microscope with differential interference contrast. Two specimens were prepared for transmission electron microscopy (TEM). The animals were preserved in 2.5% glutaraldehyde in 0.1 mol L^{-1} sodium cacodylate buffer (pH 7.3) for 24 h, rinsed in buffer (pH 7.3) for 1 h, postfixed in 1% OsO_4 for 1 h, rinsed again in buffer, and dehydrated in series of alcohols (50%, 70%, 90%, 95%) for 15 min and then 100% for 30 min (twice). The specimens were next processed through a series of ethanol: Spurr's low viscosity resin in proportions of 3:1 (4 h), 1:1 (20 h), and 1:3 (4 h) on a slow rotator at room temperature. They were transferred to pure resin (2 h) and then transferred again to pure resin and embedded in 00 BEEM capsules® for 24 h in a 60° C oven. Blocks were trimmed and then sectioned on a Leica UC7® ultramicrotome with a diamond knife (DIATOME®). Once the gland was located in section, we proceeded to section the animal to get the best orientation of the gland and its duct, the latter of which was often curved in fixed animals (Figure 1a,b). Sections were collected on gold grids and stained with uranyl acetate (2 min) and lead citrate (2 min). Digital photographs were taken on a Philips CM10® TEM at 80 kV equipped with a side-mounted Gatan Orius® digital camera. Illustrations of the gland sections were based on these digital images (Figure 1c–h). Measurements of organelles were made using Fiji (*ImageJ*, v2.1.0/1.53c) and include means ± one standard deviation. Digital photographs were edited using Adobe Photoshop® (Release 22.5, 1990–2021).

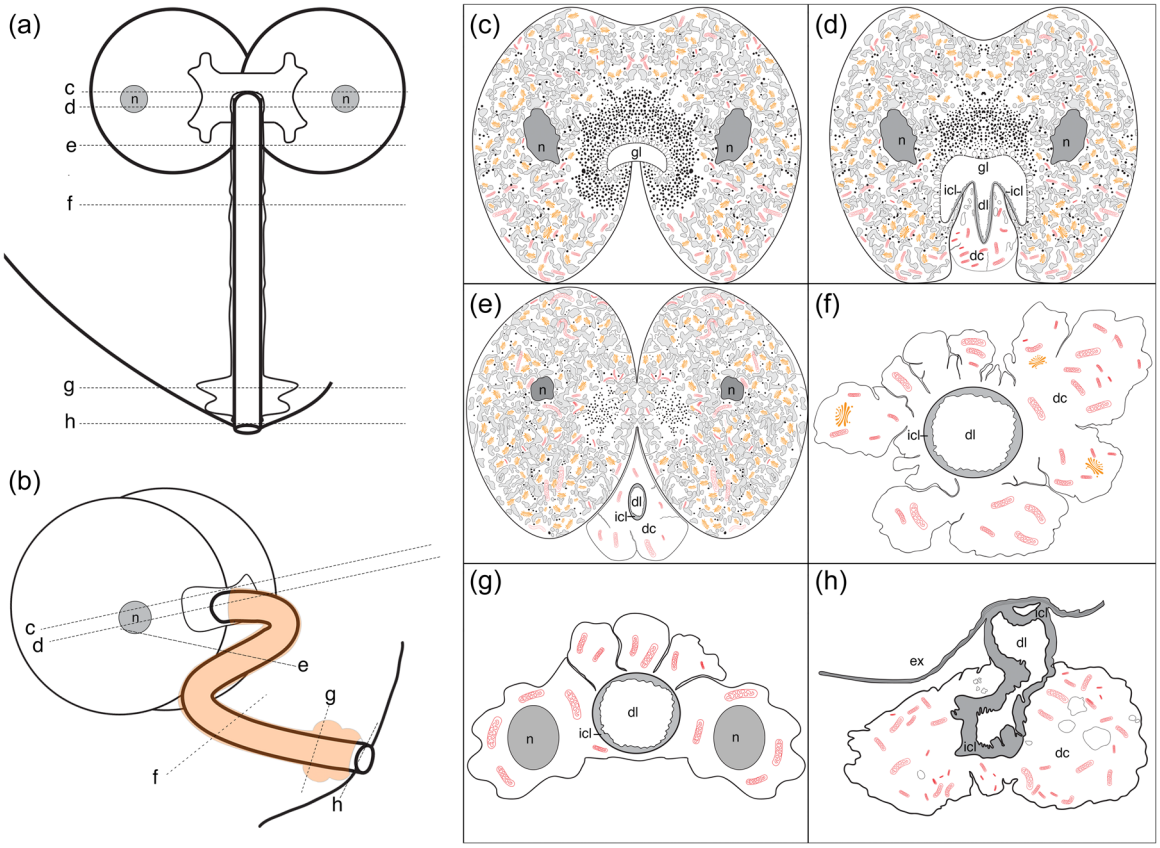

FIGURE 1 Schematics of transmission electron microscopy sections taken through the pedal gland and duct of *Asplanchna* aff. *herricki*. (a, b) Illustrations of the gland and duct and the orientation of sections taken through them. (c) Section through entire gland corresponds closely with Figure 3. (d) Section through the gland where the gland and duct lumena are confluent. This schematic corresponds closely with Figure 7a. (e–h) Sections through the gland duct that correspond closely with Figure 7b–f. dc, duct cell; dl, duct lumen; ex, external environment; ICL, intracytoplasmic lamina of the integument; gl, gland lumen; n, nucleus.

3 | RESULTS

3.1 | Gross anatomy

The pedal gland appears as a paired structure (i.e., pedal glands) on the ventroposterior margin of the animal (Figure 2a; Video S1). Close inspection reveals it to be a single, syncytial organ with two nucleated bodies and a single duct (Figure 2a–f; Video S2). The entire gland was approximately 80 µm in diameter and granular in appearance with light microscopy (Figure 2c,f). The singular duct was made up of at least two syncytial cells that extended from the base of the gland (at the midline) and fused with the integument (Figure 2d–f). Mucus-like gel extended from the duct (Figure 2f) and formed long strings (Figure 2g,h; Video S3).

3.2 | Gland ultrastructure

The entire gland was surrounded by a single uninterrupted plasma membrane (Figure 3). It was entirely syncytial: that is, there was no evidence of plasma membranes in the center of the complex that would signify two separate glands (Figure 3). There was no basal lamina around the gland complex though some whisps of glycocalyx-like material was occasionally present. The complex contained abundant rER, which appeared as a network of swollen cisternae from the periphery of the complex to its core (Figure 4a–d). The cisternal swellings were only characteristic of the rER and not observed in the mitochondria or Golgi of the gland, nor was there any evidence of swelling in the rER of other organs including the gastric glands, protonephridia, and vitellarium of the same specimens (Figure 5a–e). The swollen rER was present in several distended shapes and intracisternal widths varied from 217 to 953 nm ($\bar{x} = 453 \pm 217$ nm; $n = 17$). The lumena of all cisternae were mostly electron lucent but still had a mottled appearance that may be indicative of intracisternal proteins. The plasma membranes were all coated with ribosomes (arrowheads, Figure 4b) and there was no evidence of smooth endoplasmic reticulum anywhere in the gland.

Mitochondria were numerous and distributed between rER cisternae (Figure 4c). The cytosol surrounding the rER and mitochondria was more electron dense than the rER lumena and had a similar stippled appearance (Figure 4b,c): the resolution was not

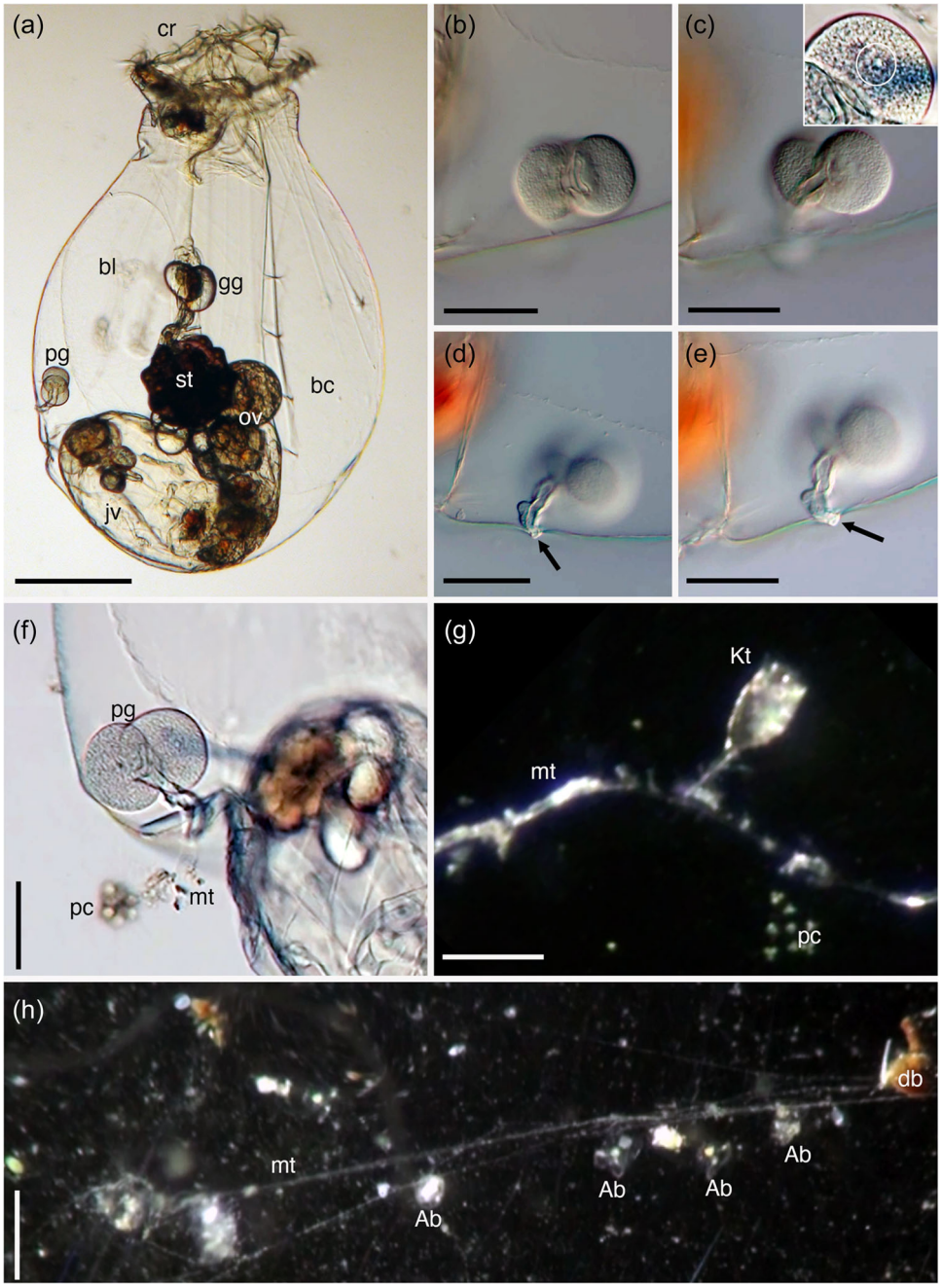

FIGURE 2 Light micrographs of *Asplanchna* aff. *herricki* and the functioning pedal gland. (a) Brightfield micrograph of an adult female. (b–e) Series of brightfield focal planes on the pedal gland showing the gland cell body and singular duct. (c) A single nucleus (white outline) in one-half of the pedal gland body. Black arrows point to the gland tube extending slightly beyond the integument. (f) Close-up of the pedal gland showing a short mucus thread and affiliated debris. (g) Stereomicroscope view (reflected light) showing a portion of a mucus thread with a rotifer (*Keratella*) and protist colony attached. (h) Long mucus thread viewed under reflected light. Several individuals of *Asplanchna* aff. *herricki* have settled on the mucus thread; it also has debris attached. Ab, individual *A.* aff. *herricki*; bc, body cavity; bl, bladder; cr, corona; db, debris; gg, gastric gland; jv, juvenile developing in utero; Kt, species of *Keratella* (rotifer); mt, mucus thread; ov, developing asexual ovocytes; pc, protist colony; pg, pedal gland; st, stomach. Scale bars: (a) 250 μm; (b–e) 63 μm; (f) 50 μm; (g) 90 μm; (h) 900 μm.

adequate to determine whether glycogen, ribosomes, or polyribosomes were the sources of the electron density.

Golgi was abundant throughout the cytosol from the periphery to the interior of the gland. Cisternae were stacked four to six deep (Figure 4c,d) and varied in length from 1184 to 1997 nm ($\bar{x}$ = 1461 ± 332 nm; n = 21). Intracisternal lumena were electron dense. Pre-Golgi intermediates (pGis) on the *cis* face (entry face) of the Golgi were difficult to identify due to the proximity of rER and the density of the cytosol. In the few sections where they could be identified, pGi vesicles were electron opaque and 30–52 nm in

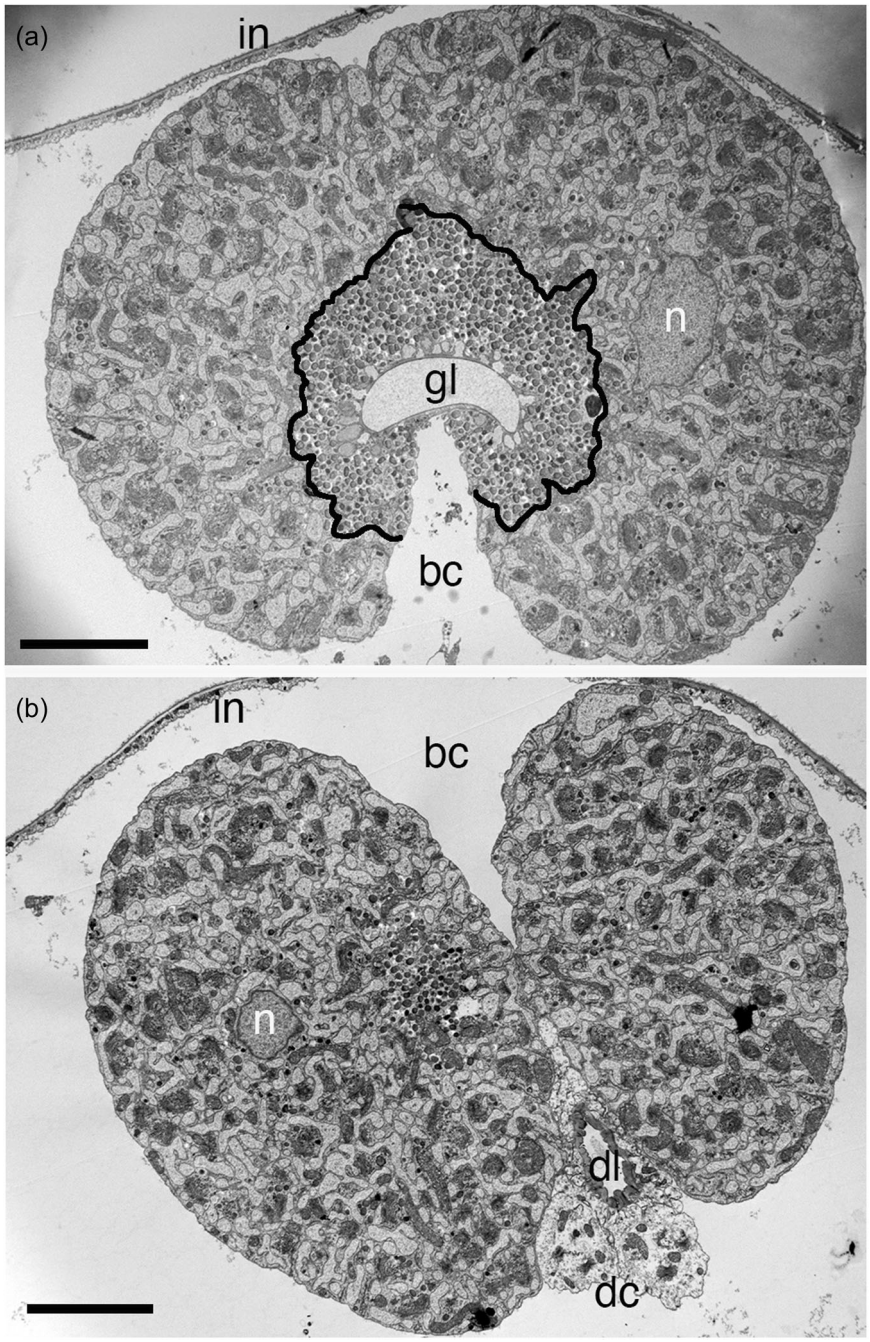

FIGURE 3 Whole sections of the pedal gland from one specimen of *Asplanchna* aff. *herricki* viewed with transmission electron microscopy. (a) Cross section of the gland before it merges with the duct. The black outline shows the collection of membrane-bound secretory vesicles near the gland lumen. (b) Section of the gland with a fold of duct at its base. bc, body cavity of adult female; dc, duct cell; dl, duct lumen; gl, gland lumen; in, integument; n, nucleus. Scale bars: (a, b) 8.5 μm.

diameter ($\bar{x}$ = 40 ± 6 nm, *n* = 5) (Figure 4e). Condensing vesicles (i.e., immature secretory vesicles) proximal to the *trans* face (exit face) were generally more numerous and often more electron dense (Figure 4d,f,g). Vesicle size was 45–97 nm ($\bar{x}$ = 62 ± 15 nm, *n* = 18). In some sections, dilations of the *trans* Golgi cisternae could be observed in the process of producing condensing vesicles (Figure 4g). Larger electron-dense secretory granules (Type 1 vesicles) were present throughout the cytosol (Figure 6). All secretions were round to oval and had a thin outline that presumably corresponded to a membrane. Some mature secretory granules near the periphery of the glands were scattered throughout the cytosol between rER cisterna and around the nuclei (Figure 6b). Vesicles varied in size from 169 to 382 nm ($\bar{x}$ = 291 ± 66 nm; *n* = 31). Numerous Type 1 secretory vesicles clumped together closer to the midline of the gland (Figure 6c,d). These vesicles were of similar electron density to those around the gland periphery but were often slightly larger in diameter (298–553 nm, $\bar{x}$ = 385 ± 68 nm; *n* = 24).

A variety of small (<50 nm diameter) vesicles were scattered among the mature secretory vesicles. These tiny vesicles were never near Golgi cisternae and some had peculiar shapes and contents that were either electron dense or electron lucent (*Figure 6c,d). A series large membrane-bound vesicles (Type 2) of variable shape were clustered near the midline of the gland complex and proximal to the aggregations of Type 1 vesicles (Figures 3, 4, and 6f–h). The bounding

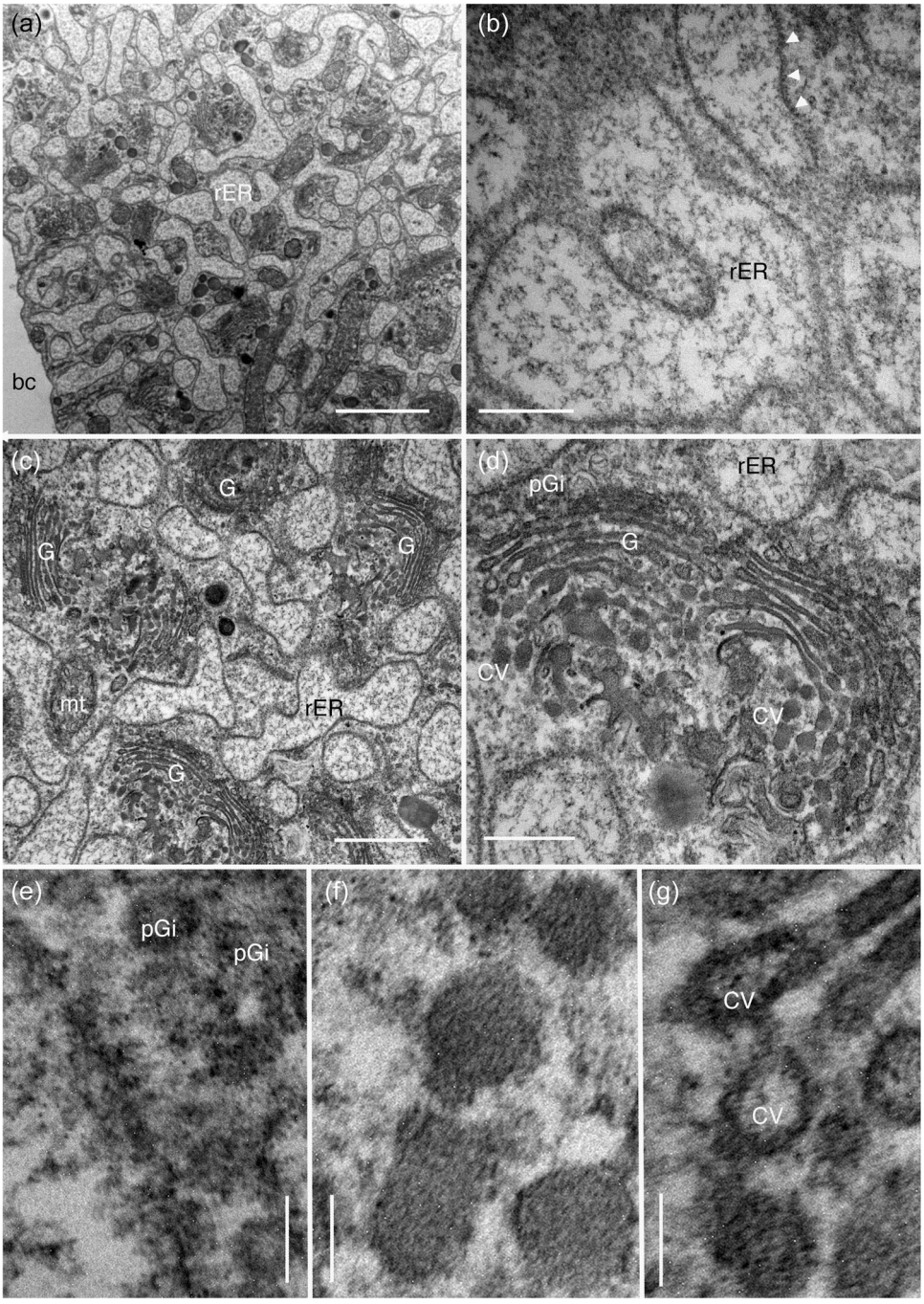

FIGURE 4 Close-up of the organelles in the pedal gland of *Asplanchna* aff. *herricki* viewed with transmission electron microscopy. (a) Gland periphery showing the abundant rough endoplasmic reticulum (rER) with electron-lucent lumena. (b) Magnified view of the rER revealing its contents and dilated appearance. White arrowheads point to electron-dense dots (ribosomes) along the rER membrane. (c) Abundant Golgi and rER cisternae. (d) Closeup of the Golgi revealing the pre-Golgi intermediates and the production of condensing vesicles (CV) from the Golgi cisternae. (e) Magnified view of the pre-Golgi intermediates (pGi). (f, g) Close-up of CV free in the cytosol and under production from the cisternae. bc, body cavity of the adult female; G, Golgi cisternae; mt, mitochondria; rER, rough endoplasmic reticulum. Scale bars: (a) 2 μm; (b) 200 nm; (c) 500 nm; (d) 200 nm; (e) 70 nm; (f) 80 nm; (g) 70 nm.

membranes were electron-dense and the lumen contents generally consisted of electron-dense fibers (Figure 6a,e–h), but in some cases, they contained other undetermined structures that may be membrane-bound (asterisk, Figure 6e). Measurements of the vesicles (along their longest sides) showed a range of sizes from 420 to 822 nm ($\bar{x}$ = 632 ± 108 nm; n = 13). Many of these vesicles appeared to fuse with the intracytoplasmic lamina (ICL) and plasma membrane that lined gland lumen (Figure 6d,e). Fusion pores in the plasma membrane were 128–149 nm ($\bar{x}$ = 137 ± 10 nm; n = 7). Exocytosis of vesicle contents to the gland lumen was present in all examined sections (Figure 6g,h).

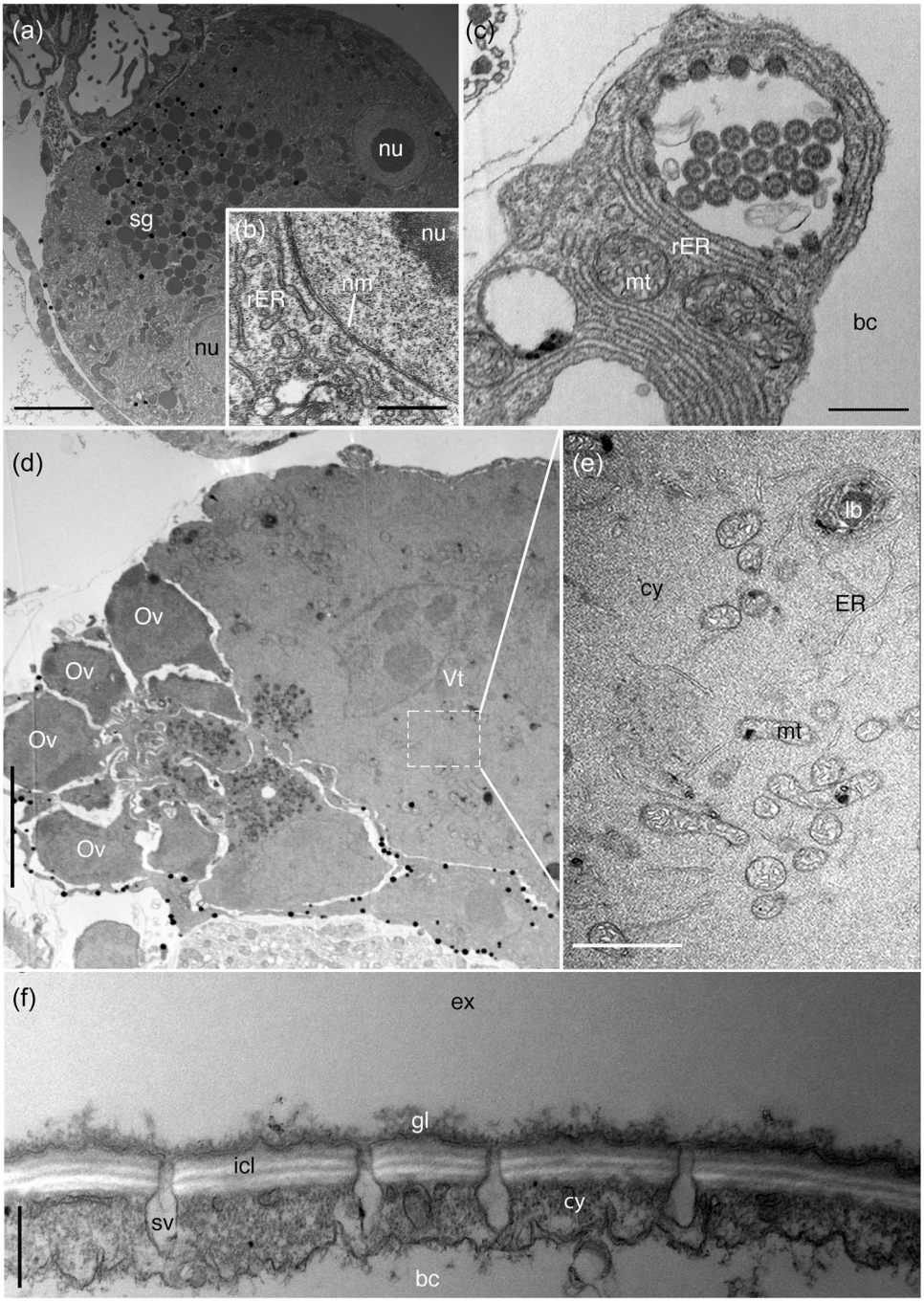

FIGURE 5 The ultrastructure of other syncytial organs in *Asplanchna* aff. *herricki* for comparison to the pedal gland. (a) Gastric gland. (b) Magnified view of the nucleus and nondilated rough endoplasmic reticulum (rER) in the cytoplasm of the gastric gland. (b) Protonephridium. (d) Low magnification view of the germovitellarium. (e) Closeup of the vitellarium cytoplasm showing nondilated rER. (f) Integument of the trunk. bc, body cavity; cy, cytoplasm; ER, endoplasmic reticulum; ex, external environment; gl, glycocalyx; ICL, intracytoplasmic lamina; mt, mitochondria; nm, nuclear membrane; nu, nucleus; ov, ovocytes; sg, secretory granules; sv, secretory vesicle; vt, vitellarium; Scale bars: (a) 8 μm; (b) 6 μm; (c) 400 nm.

A large lumen was present at the midline of the gland where the nucleated bodies fused with the duct cells (Figures 3 and 7a). The gland lumen was an enclosed space that fed directly into the lumen of the duct. The shape of the gland lumen was generally oval and approximately 1.7 × 4.5 μm (24 μm^2). The gland lumen was lined with integument that contained a smooth ICL that appeared as a relatively homogeneous electron-opaque region (Figure 6g,h). The ICL was 127–327 nm thick ($\bar{x}$ = 251 ± 62 nm; n = 14); the trilaminar plasma membrane was 31–39 nm thick ($\bar{x}$ = 34 ± 3 nm; n = 8). The ICL showed evidence of vesicle fusion around its perimeter (Figure 6g,h). The contents of the gland lumen had a fine mesh-like appearance that resembles contents of Type 2 vesicles (Figure 6g,h).

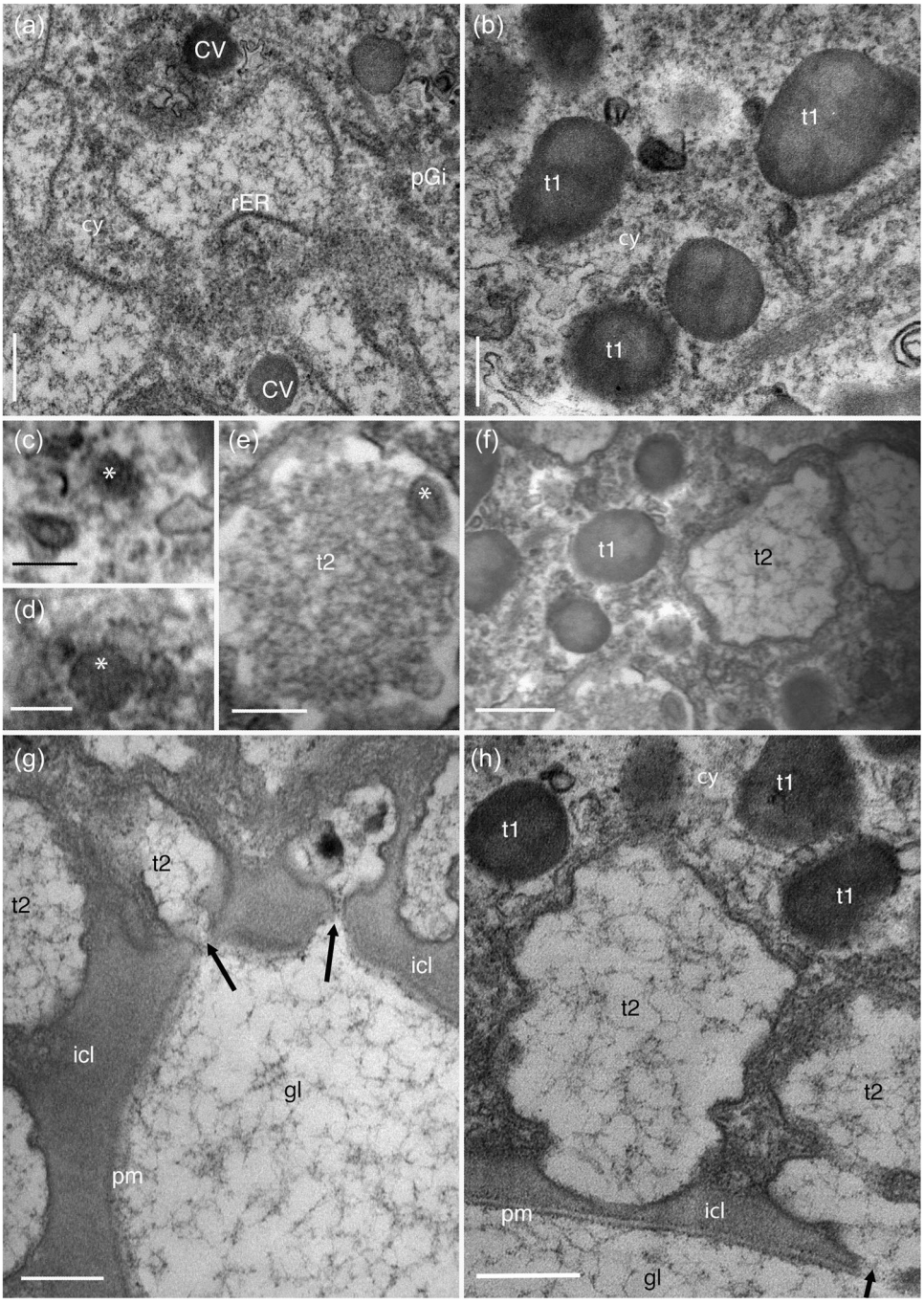

FIGURE 6 Ultrastructure of the pedal gland of *Asplanchna* aff. *herricki*. (a) Condensing vesicles near the rough endoplasmic reticulum. (b) Type 1 secretory vesicles with their electron-dense contents. (c, d) Magnified views of very small vesicles scattered around the Type 2 secretory vesicles near the gland lumen. (e) Mesh-like contents of a Type 2 secretory vesicle and an unidentified vesicle-like structure (*) inside the larger vesicle. (f) Types 1 and 2 secretory vesicles. (g) Magnified view of fusion pores (arrows) created by the Type 2 vesicles and their interaction with the integument lining the gland lumen. (h) Close-ups of Type 2 secretory vesicles and their contents, which are similar to the contents in the gland lumen. *Unidentified vesicles; cv, condensing vesicles; gl, gland lumen; ICL, intracytoplasmic lamina of the integument; pm, plasma membrane; pGi, pre-Golgi intermediates; rER, rough endpoplasmic reticulum; t1, Type 1 secretory vesicle; t2, Type 2 secretory vesicle. Scale bars: (a) 70 nm; (b) 250 nm; (c) 80 nm; (d) 90 nm; (e) 100 nm; (f) 300 nm; (g) 250 nm; (h) 150 nm.

3.3 | Duct ultrastructure

The gland appeared to fuse with a series of duct cells close to its midline (Figure 7a). Duct cells could be differentiated from the gland syncytium by their cellular contents, the more electron-lucent cytoplasm, and the structure of their ICL. Where the duct cells fused with the gland syncytium (observed in longitudinal section only; Figure 7a), the cytoplasm became noticeably more

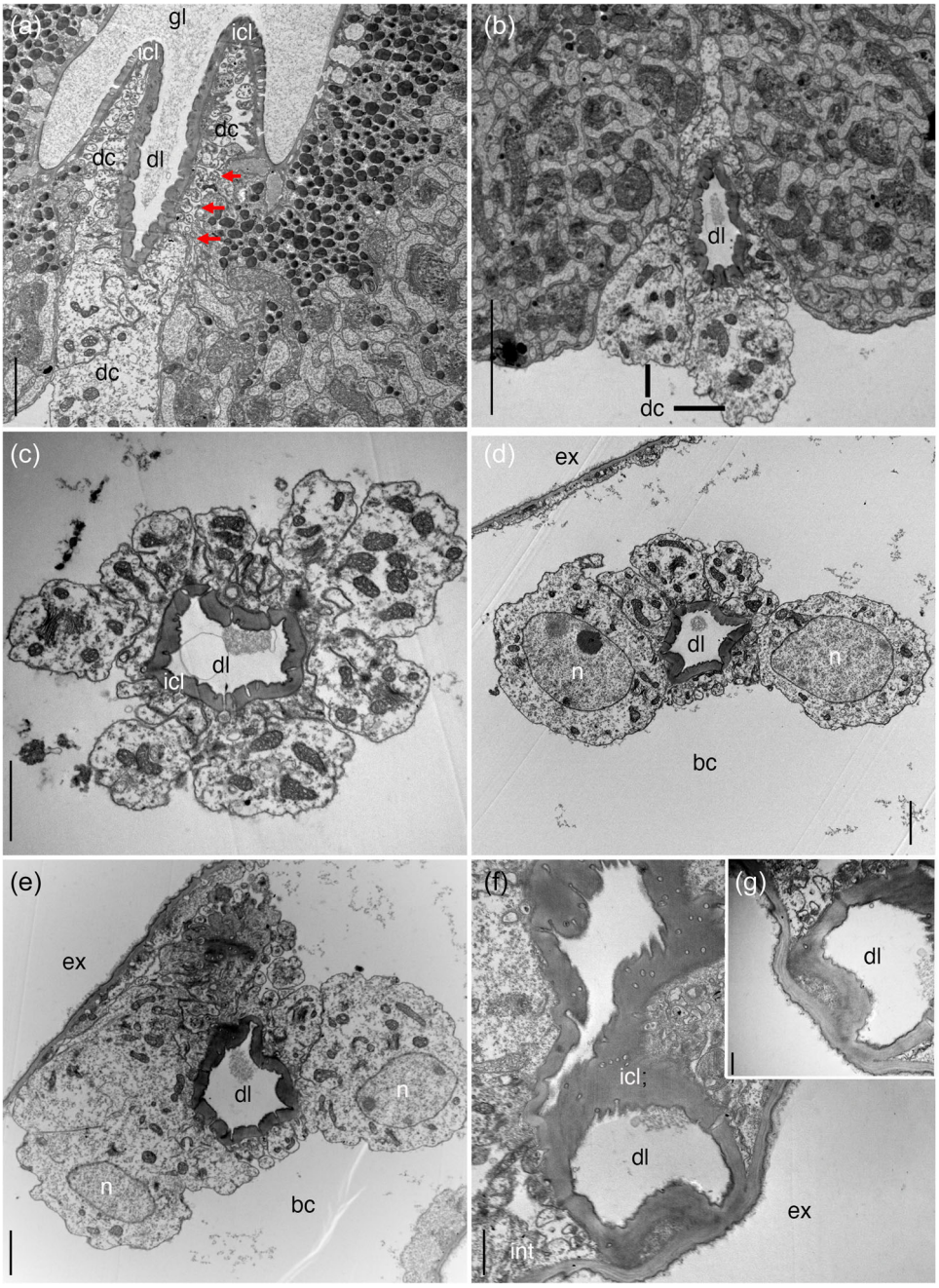

FIGURE 7 Pedal gland and duct of *Asplanchna* aff. *herricki*. (a) Fusion of the gland lumen with the duct lumen. Note that the cytoplasm of the duct cells is more electron lucent that the cytoplasm of the gland cell. A plasma membrane separates much of the duct cell from the gland cell but appears to disappear (red arrows) in some areas where it meets the gland cell body. (b) Cross section of a bent duct directly beneath the gland; (c) cross section of the gland duct approximately halfway down its length; (d) cross section of gland duct showing the two nuclei; (e) cross section of the gland duct where it fuses with the integument; (f) tangential section where gland duct fuses with integument, showing the confluence of the intracytoplasmic lamina of both regions. (g) Same approximate region as (f) but in near cross section. Red arrows, region where no plasma membrane can be observed between duct cells and gland; bc, body cavity; dc, duct cell; dl, duct lumen; ex, external environment; gl, gland lumen; icl, intracytoplasmic lamina of the integument; int, integument; n, nucleus. Scale bars: (a) 200 nm; (b) 7 μm; (c) 2.5 μm; (d) 2 μm; (e) 3 μm; (f) 8.3 μm; (g) 6 μm.

electron lucent, there were no secretory vesicles, and the ICL contained many deep furrows (resembling the ICL at the base of the duct where it met the body wall; Figure 7f). A plasma membrane could be observed between the duct cells and the gland syncytium for most of its length; however, where the apical end of the duct met the gland, no plasma membrane could be discerned (arrows, Figure 7a), and so there may be cytoplasmic continuity between the gland syncytium and duct cell cytoplasm. The ICL of the duct lumen was similar in staining quality to the ICL of the gland lumen but often had a slightly more electron-dense base and was always thicker and highly folded: 115–835 nm thick ($\bar{x}$ = 343 ± 178 nm; n = 15).

The remainder of the duct below the gland was only observed in cross section (Figure 7b–f). Where the gland lumen fed into the duct, the area of the duct lumen expanded to 25 μm^2; about halfway down the length of the duct the lumen expanded to about 37 μm^2, which then narrowed toward the base to an area of 20 μm^2. The ICL had a similar thickness at the top and bottom of the duct. The number of cells that made up the duct was difficult to count accurately because their plasma membranes were highly folded and gave the impression of multiple cell bodies though only two nuclei were ever observed (see below). The cytosol always contained mitochondria but relatively few cisternae of rER and Golgi. At the base of the duct but before it fused with the integument were two nuclei 5.6–5.7 µm diameter, which corresponded in number, size, and position to the nuclei that were observed with light microscopy (Figure 2). The cytoplasm around these nuclei was generally more mottled than the cytoplasm along the duct's length. The width of the duct at this section was about 21 µm.

The duct fused with the posterior body wall to form a duct opening. The ducts cells had cytoplasmic continuity with the integument (Figure 7f,g). Evidence of this was not always obvious, but the intracytoplasmic lamina of both the inner duct lumen and the external integument was continuous. In fact, the uneven (furrowed) nature of the ICL in the duct lumen was also observed in the integument around the duct opening but nowhere else on the trunk (Figure 5f). The ICL of the duct integument often had small cavities in it (Figure 7f) that were reminiscent of exocytic vesicles present in the ICL at the top of the duct. Such cavities were absent from the ICL of the integument, though secretory vesicles were present (Figure 5f). The ICL of the integument also consisted of numerous laminae that were not observed in the ICL of the duct.

4 | DISCUSSION

4.1 | Rotifer pedal glands

Rotifers are peculiar micrometazoans owing to their eutelic bodies and propensity for organ systems to comprise a mixture of cellular and syncytial tissues (Clément & Wurdak,1991; Fontaneto & De Smet, 2014; Hyman, 1951). Early studies recognized these qualities (van Cleave, 1932; Hickernell, 1917; Montgomery, 1903; Remane, 1933; Hyman, 1951), but also discovered that despite them, rotifer morphology can be extremely complex (Hyman, 1951; Remane, 1933). Knowledge of this complexity has increased over the past several decades as studies of organ system ultrastructure became more common, ultimately being summarized in the excellent series *Microscopic Anatomy of Invertebrates* (Clément & Wurdak, 1991). While that work provided a comprehensive overview of the ultrastructure of most rotifer organ systems, information on exocrine glands was relatively scant (Clément & Wurdak, 1991). The reasons for this might be varied, but it ultimately left a knowledge gap of some anatomical structures that play important roles in rotifer life history and that also have value in understanding rotifer systematics and evolution.

Female rotifer exocrine glands are present in four to five general varieties defined by their position or function in the body: cellular pedal and style glands in the foot region; syncytial trunk glands, syncytial salivary glands, and retrocerebral glands in the head. The pedal glands function to secrete adhesives from the foot (Dickson & Mercer, 1966; Fontaneto & De Smet, 2014) and/or build extracorporeal tubes around the bodies of some sessile, adult females (Clément & Wurdak, 1991; Yang & Hochberg, 2018a, 2018b; Yang et al., 2021). They also may play a role in binding eggs to the body of ovigerous species as do style glands (Gilbert, 1988; Sudzuki, 1957a, 1957b). The trunk glands are part of the syncytial integument and appear to function in the secretion of specific parts of the hardened tubes of some sessile rotifers (Yang & Hochberg, 2018b). Salivary glands connect to the mastax and were originally thought to function as endocrine organs, releasing their substances to the internal jaws (Clément & Wurdak, 1991; Štrojsová & Vrba, 2007); however, studies by Balazs et al. (2021) and Datki et al. (2021, 2022a, 2022b, 2023) suggest they may also function in an exocrine fashion, releasing a thread-like biopolymer to the external environment that functions for feeding. Retrocerebral glands may be cellular or syncytial and function to secrete either a mucus that acts as a lubricant for the corona or as an adhesive for egg attachment (Fontaneto & De Smet, 2014; Hochberg et al., 2023). Of the five gland types, species of *Asplanchna* generally only possess salivary glands (Wurdak, 1987). However, *A. herricki* Guerne, 1888 is known to possess pedal glands, and so differs considerably from all other members of the genus. In this study, we describe the pedal gland of a species' morphotype we call *A.* aff. *herricki*, which is similar to the type (de Guerne, 1888) and subsequent descriptions (Koste, 1978; de Paggi, 2002; Wierzejski, 1893) but with some exceptions that might be part of the species' natural variation or may indicate that it is a member of a cryptic species complex. The pedal gland in *A.* aff. *herricki* is a syncytial organ that may be derived from similar, albeit cellular, pedal glands present in the sister group *Asplanchnopus* and potentially in the common ancestor (Walsh et al., 2005).

Taxonomic diagnoses of *Asplanchna* state that species of this lineage lost their foot, toes, and affiliated pedal glands during their evolution (de Paggi, 2002; de Paggi et al., 2020; Shiel & Koste, 1993). Species of related taxa in family Asplanchnidae—*Asplanchnopus* and *Harringia*—all possess a foot, toes, and paired pedal glands, and this is reflected in the latest phylogeny of the family Asplanchnidae (Walsh et al., 2005). Despite this, a species described over a century ago—*A. herricki*—and redescribed not long after (Wierzejski, 1893), was reported to have paired pedal glands. While detailed photographs were never provided, subsequent illustrations and taxonomic diagnoses have described an animal with rudimentary toes and paired pedal glands fused along their midline (de Paggi, 2002). These glands were assumed to be vestigial (de Paggi, 2002). This hypothesis is presumably derived from an absence of observations of any secretions from the glands but may also be built out of bias: the reduction of the foot and toes and their presumable nonfunctional nature led to the assumption that the gland(s) were also nonfunctional by association.

4.2 | Pedal gland ultrastructure and secretion

The pedal gland of *A.* aff. *herricki* appears at the gross morphological level to consist of two fused gland cells that channel their secretions into a singular duct. In general, rotifer pedal glands are single cells and do not have separate cellular ducts for releasing their secretions to the external environment (Clément & Wurdak, 1991; Dickson & Mercer, 1966). Instead, gland ducts are merely extensions of the individual gland cell bodies that direct their secretory vesicles out the foot and toes via exocytosis (Dickson & Mercer, 1966; Yang et al., 2021). The plasma membranes of the gland cells may be reinforced with microtubules to stabilize the cells during the extrusion process (Dickson & Mercer, 1966). The gland of *A.* aff. *herricki* is unlike these other glands: it is a syncytial organ that may be derived from the fusion of two glands during embryogenesis (based on shape of the organ and the presence of two nuclei), while the duct appears to be a derivative of the posterior integument and is free of microtubules.

The pedal gland is not invested with any muscles nor is it obviously innervated. The gland also does not possess a reservoir for the collection of secretory products as is the case for the retrocerebral glands of some rotifers (Fontaneto & De Smet, 2014; Hochberg et al., 2023). The pedal gland appears to engage in regulated secretion, whereby the secretory granules are stored in the cytosol and then exocytosed into the gland lumen upon stimulation (Burgess & Kelly, 1987; Hochberg et al., 2023). At the ultrastructural level, the secretory process appears to be straightforward: rER provides pGis to the *cis* side of Golgi cisternae, which then modifies the secretion before releasing them as condensing vesicles (e.g., immature secretory vesicles) to the rest of the cytosol. From here, the immature vesicles appear to fuse forming a larger electron-dense secretory vesicles (Type 1), though fusion was not observed in our material. These vesicles may be stored for some time as they tend to be distributed throughout the cytosol: many also accumulate near the center of the gland close to the lumen. The fate of these vesicles is uncertain, but we envision three scenarios based on contents inside the gland and duct lumen (Figure 8). (1) Type 1 vesicles

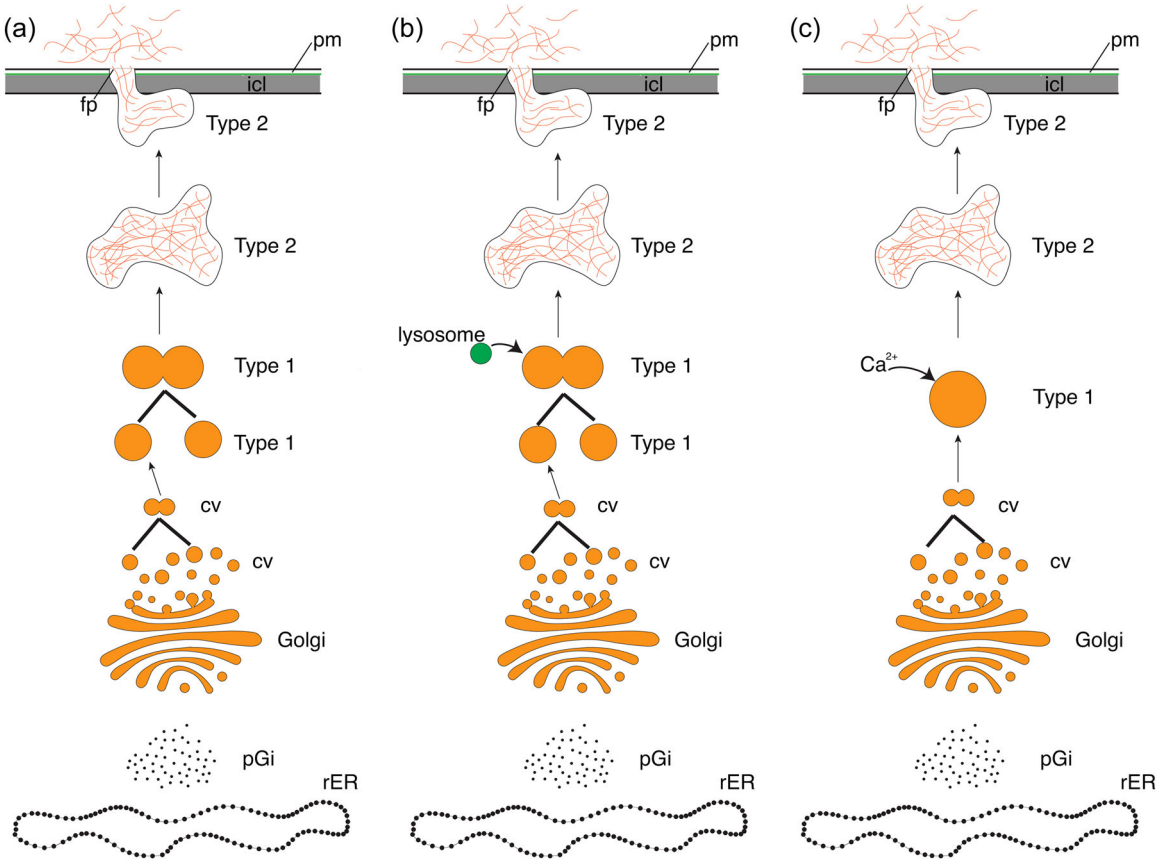

FIGURE 8 Three hypothetical secretory pathways for the mucus in the pedal gland of *Asplanchna* aff. *herricki*. All pathways involve fusion of condensing vesicles (cv) into Type 1 vesicles. The differences between the proposed pathways involve how Type 1 vesicles transform into Type 2 vesicles, which may also affect how their contents transition from condensed to decondensed. All Type 2 vesicles appear to engage in a form of kiss-and-run exocytosis sensu Rutter and Tsuboi (2004). (a) This pathway involves homotypic fusion of Type 1 vesicles to eventually produce a Type 2 vesicle. The fusion may lead to decondensation of the contents. (b) This pathway involves homotypic fusion of Type 1 vesicles that combine with a lysosome (not observed in sections) to create a Type 2 vesicle with its decondensed contents. (c) This pathway involves an intracellular signal such as Ca^{2+} that leads to radial expansion of Type 1 vesicles followed by decondensation of their contents. Additional explanations in the text. fp, fusion pore; ICL, intracytoplasmic lamina of the integument; pGi, pre-Golgi intermediates; pm, plasma membrane that lines the integument of the pedal gland lumen; rER, rough endoplasmic reticulum.

fuse (homotypic fusion: Hochberg et al., 2023) to create a new membrane-bound vesicle (Type 2). Fusion of two or more Type 1 vesicles leads to remodeling of the plasma membranes to create the larger Type 2 vesicles. Remodeling of vesicle contents may occur through lumenal acidification or enzymatic hydrolysis to process pro-proteins, which is a common process before exocytosis in vertebrate animals (Mellman et al., 1986): in the case of *A.* aff. *herricki*, remodeling of the e-dense secretory granule leads to a phase transition that transforms the contents into mesh-like network of fibers characteristic of Type 2 vesicles (Figure 8a). Type 2 vesicles are now mature secretory granules with contents that match those in the gland and duct lumens. (2) Type 1 vesicles fuse with an as-yet unidentified vesicle (possibly a lysosome) to create the mature Type 2 vesicle, which also expands in size but remodels its contents through lysosomal secretions before exocytosis (Figure 8b). (3) In the absence of homotypic fusion, individual Type 1 vesicles received an intracellular signal (e.g., Ca^{2+}, Figure 8c) that causes swelling of the condensed matrix inside Type 1 vesicles, thereby leading to radial expansion of the plasma membrane and a phase transition of the internal granule from condensed to decondensed (Chin et al., 2004). This type of polymer gel phase transition is characteristic of mucins that are stored in secretory granules (Verdugo, 2005). At present, we do not know which process is characteristic of the pedal gland of *A. aff. herricki*.

Exocytosis of the gland contents initially appears to follow the "kiss-and-run model" (Houy et al., 2013; Rutter & Tsuboi, 2004); that is, in many vertebrate cells, a secretory vesicle forms only a small fusion pore with the plasma membrane of a lumen to release the contents. Evidence for this comes from the fact that only small fusions pores were ever observed in our material. The alternative mechanism is full fusion exocytosis, wherein a vesicle membrane collapses into and becomes part of the plasma membrane of the lumen (Pavelka & Roth, 2015). In this case, the newly formed membrane would continue to expand unless the old membrane was removed via clathrin-mediated endocytosis: that is, pieces of the plasma membrane are retrieved in a piecemeal fashion (Brown, 1989; Meldolesi & Ceccarelli, 1981; Pavelka & Roth, 2015). Evidence for this process is observed in the cytosol around Type 2 vesicles near the gland lumen, where small vesicles are present (see Figure 6c,d). We are uncertain if both processes can happen in the same cell, or if we are misinterpreting our micrographs.

The secreted contents of the gland flow down the duct lumen and out the duct pore. Interestingly, the duct lumen has a thick intracytoplasmic lamina (115–835 nm thick; $\bar{x}$ = 343 ± 178 nm) relative to the ICL of the body wall (47–125 nm; $\bar{x}$ = 99 ± 24 nm). The functional significance of this is unknown, but the thick ICL may act as reinforcement for the duct to prevent kinking and blockage of flow (though it can bend) during body contractions. Pedal gland cells in other rotifers have plasma membranes reinforced with fibers for presumably a similar function (Dickson & Mercer, 1966). Our observations suggest the duct itself is a derivative of the body wall and probably develops as an invagination during embryogenesis. The cytoplasmic contents are similar between duct and body wall integument, though the latter has a darker cytosol and the ICL is more laminated in appearance.

4.3 | Function of the mucus

Results of this study suggest that the pedal gland of *A.* aff. *herricki* is functional and engages in secretion following a synthetic pathway that may involve homotypic fusion of secretion granules followed by exocytosis (Hochberg et al., 2023). What remains to be determined is the function of the secreted matrix. Not all *A.* aff. *herricki* secreted the mucus during our observations, but when it was present, it remained attached to the animal for several hours. In one case, a rotifer left overnight in a small bowl was unattached from the mucus the following day, which remained suspended in the water. We entertained the possibility that this mucus functions to collect prey as the rotifers glide through the water, similar to the way some dinoflagellates collect prey (Kiφrboe & Titelman, 1998). In all instances where rotifers had extruded a thread-like mucus secretion, there were always algae, protists, and/or other rotifers (e.g., *Keratella*) attached to it (Figure 2g,h; Video S3). This could be coincidental rather than a feeding strategy. We never observed *A.* aff. *herricki* turning around and feeding on either the prey or the mucus string; this argues against the mucus function as a prey trap. We also considered the possibility that formation of a mucus string was artificial: that is, a result of unusual water chemistry having some sort of osmotic effect on the glands. This seems unlikely because we only used native pond water and not all rotifers secreted the mucus when in the same bowl of water. Mucus secretion was not constant, but we do not know the stimulus for secretion when it was present. Perhaps secretion is a function of mechanical disturbance as proposed for other rotifers that secrete biopolymers from their salivary glands (Datki et al., 2021, 2022a, 2022b, 2023).

Our observations do not clearly support the hypothesis that mucus production functions for attachment to a substratum as it does for the pedal glands of other rotifers; however, more observations are needed. While we never observed a rotifer attaching to the sides of the experimental vessel or any submerged materials, we did observe conspecifics attaching to another specimen's mucus thread to form pseudoaggregations. This attachment and clumping may or may not be natural: that is, we do not know whether or not this happens in nature or is an artificial behavior due to multiple rotifers (n = 4) swimming together in a small volume (5 mls) of pond water. It was interesting to note that attachment by conspecifics was not obviously accidental as they all attached with their posterior ends (where a foot would be present if they had one). Beyond this, we were unable to determine whether, and why, conspecifics would attach, and we never observed conspecifics detaching from the thread over the course of several hours. Regardless, we think the mucus can play a role in attachment. We can foresee its utility in forming a sort of anchor to a nearby object—floating vegetation—allowing an animal to remain somewhat stationary in the plankton

(Hampton et al., 2000) and perhaps take advantage of a static cloud of prey (similarly hypothesized for *Plationus patulus*: Hampton & Gilbert, 2001). The gland may also allow for temporary attachment to a substrate while it oviposits. Alternatively, the mucus may function for buoyancy as it does for larvae of the annelid *Poecilochaetus serpens* Allen, 1904 that secretes mucus to suspend themselves in the plankton with relatively little energy expenditure (Nozais et al., 1997).

4.4 | Future directions

The chemical ecology of rotifers was reviewed by Snell (1998) who examined how rotifers respond to chemical cues in their environment, some of which were produced by the rotifers themselves for mating and defense. In Snell's review, rotifers were only observed to secrete minute amounts of chemicals and nothing like the copious secretions known for the species observed by Balazs et al. (2021) and Datki et al. (2021, 2022a, 2022b, 2023) or by us with *A.* aff. *herricki*. Among invertebrates, reports of suspended mucus secretions come mostly from observations of larger animals such as corals (Goldberg et al., 2018), echinoderms (Nance & Braithwaite, 1979), gastropods (Kappner et al., 2000), and ascidians (Petersen, 2007) to name a few; other examples are noted in Jørgensen et al. (1984). In other microeukaryotes, such secretions are noted for algae (Chin et al., 2004) including dinoflagellates (Kiφrboe & Titelman, 1998). Most secretions from these organisms appear to be related to prey trapping, though other functions are also known or implied. In the case of rotifers that secrete mucus from their salivary glands, the function may be for exogenous degradation of potential food items (Datki et al., 2023). In *A.* aff. *herricki*, we suspect the mucus plays a role in either adhesion or floatation even if it does trap small animals and algae. Additional observations are warranted as are the need for chemical analyses that may provide some insights into the composition of the mucus as they have done for other rotifer secretions (Balazs et al., 2021; Datki et al., 2021, 2022a, 2022b, 2023; Yang et al., 2021).

AUTHOR CONTRIBUTIONS

Rick Hochberg and Thiago Q. Araújo designed the project. Rick Hochberg prepared the specimens for electron microscopy and performed TEM with Thiago Araújo. Rick Hochberg and Thiago Araújo prepared the figures. All authors wrote, edited, and approved the manuscript.

ACKNOWLEDGMENTS

We thank two reviewers for their valuable comments and recommendations that improved this manuscript. This research was funded in part by the National Science Foundation: DEB 2051684 (R. Hochberg), DEB 2051704 (E. J. Walsh & J. E. Mohl), and DEB 2051710 (R. L. Wallace). We thank the staff at the Electron Microscopy Facility at the UMASS Chan Medical School in Worcester, MA, for their assistance.

CONFLICT OF INTEREST STATEMENT

The authors declare no conflict of interest.

DATA AVAILABILITY STATEMENT

Data in the form of electron micrographs are available from the authors upon request.

ORCID

Rick Hochberg http://orcid.org/0000-0002-5567-5393
Robert L. Wallace http://orcid.org/0000-0001-6305-4776
Elizabeth J. Walsh http://orcid.org/0000-0002-6719-6883
Thiago Q. Araújo http://orcid.org/0000-0001-9325-6248

PEER REVIEW

The peer review history for this article is available at https://www.webofscience.com/api/gateway/wos/peer-review/10.1002/jmor.21765

REFERENCES

Balazs, E., Galik-Olah, Z., Galik, B., Somogyvari, F., Kalman, J., & Datki, Z. (2021). External modulation of Rotimer exudate secretion in monogonant rotifers. *Ecotoxicology and Environmental Safety*, *220*, 112399. https://doi.org/10.1016/j.ecoenv.2021.112399

Bentfeld, M. E. (1971). Studies of oogenesis in the rotifer, *Asplanchna*. II. Oocyte growth and development. *Zeitschrift fur Zellforschung und mikroskopische Anatomie*, *115*, 184–195.

Brown, D. (1989). Membrane recycling and epithelial cell function. *American Journal of Physiology-Renal Physiology*, *256*(1), F1–F12.

Burgess, T. L., & Kelly, R. B. (1987). Constitutive and regulated secretion of proteins. *Annual Review of Cell Biology*, *3*(1), 243–293.

Chin, W. C., Orellana, M. V., Quesada, I., & Verdugo, P. (2004). Secretion in unicellular marine phytoplankton: Demonstration of regulated exocytosis in *Phaeocystis globosa*. *Plant and Cell Physiology*, *45*(5), 535–542.

van Cleave, H. J. (1932). Eutely or cell constancy in its relation to body size. *The Quarterly Review of Biology*, *7*(1), 59–67.

Clément, P., & Wurdak, E. (1991). Rotifera. In F. W. Harrison & E. E. Ruppert (Eds.), *Microscopic anatomy of invertebrates, Volume 4: Aschelminthes* (pp. 219–297). Wiley-Liss Inc.

Datki, Z., Acs, E., Balazs, E., Sovany, T., Csoka, I., Zsuga, K., Kalman, J., & Galik-Olah, Z. (2021). Exogenic production of bioactive filamentous biopolymer by monogonant rotifers. *Ecotoxicology and Environmental Safety*, *208*, 111666.

Datki, Z., Balazs, E., Galik, B., Sinka, R., Zeitler, L., Bozso, Z., Kalman, J., Hortobagyi, T., & Galik-Olah, Z. (2022a). The interacting rotifer-biopolymers are anti-and disaggregating agents for human-type beta-amyloid in vitro. *International Journal of Biological Macromolecules*, *201*, 262–269.

Datki, Z., Darula, Z., Vedelek, V., Hunyadi-Gulyas, E., Dingmann, B. J., Vedelek, B., Kalman, J., Urban, P., Gyenesei, A., Galik-Olah, Z., Galik, B., & Sinka, R. (2023). Biofilm formation initiating rotifer-specific biopolymer and its predicted components. *International Journal of Biological Macromolecules*, *253*, 127157. https://doi.org/10.1016/j.ijbiomac.2023.127157

Datki, Z., Sinka, R., Galik, B., & Galik-Olah, Z. (2022b). Particle-dependent reproduction and exogenic biopolymer secretion of protozoa co-cultured rotifers. *International Journal of Biological Macromolecules*, *211*, 669–677.

Davies, N., Lafleur, A., Hochberg, R., Walsh, E. J., & Wallace, R. L. (2024). Key to sessile gnesiotrochan rotifers: Families, monospecific species

in Floscullariidae, species of Atrochidae, Conochilidae, and *Limnias*. *Zootaxa*, *5397*, 497–520. https://doi.org/10.11646/zootaxa.5397.4.3

Dickson, M. R., & Mercer, E. H. (1966). Fine structure of the pedal gland of *Philodina roseola* (Rotifera). *Journal of Microscopy (Paris)*, *5*, 81–90.

Ejsmont-Karabin, J. (2023). Rotifers of Lake Psammon: A knowledge synthesis. *Hydrobiologia*, *851*, 2949–2964.

Fontaneto, D., & De Smet, W. E. (2014). Rotifera. In W. Kükenthal (Ed.), *Gastrotricha and Gnathifera* (pp. 217–300). Walter de Gruyter GmbH & Co KG.

Gilbert, J. J. (1983). Rotifera. In K. G. Adiyodi & R. G. Adiyodi (Eds.), *Reproductive biology of invertebrates. Volume I. Oogenesis, oviposition, and oosorption* (pp. 181–209). John Wiley and Sons.

Gilbert, J. J. (1988). Rotifera. In K. G. Adiyodi & R. G. Adiyodi (Eds.), *Reproductive biology of invertebrates. Volume III. Accessory sex glands* (pp. 73–80). Oxford and IBH Publishing Co.

Gilbert, J. J. (1989). Rotifera. In K. G. Adiyodi & R. G. Adiyodi (Eds.), *Reproductive biology of invertebrates. Volume IV, Part A. Fertilization, development, and parental care* (pp. 179–199). Oxford and IBH Publishing Co.

Goldberg, W. M. (2018). Coral food, feeding, nutrition, and secretion: A review. In M. Kloc & J. Z. Zubiak (Eds.), *Marine organisms as model systems in biology and medicine* (pp. 377–421).

de Guerne, M. J. (1888). IV.—Monographic note on the Rotifera of the family Asplanchnidæ. *Annals and Magazine of Natural History*, *2*(7), 28–40.

Hampton, S. E., & Gilbert, J. J. (2001). Observations of insect predation on rotifers. *Hydrobiologia*, *446/447*, 115–121.

Hampton, S. E., Gilbert, J. J., & Burns, C. W. (2000). Direct and indirect effects of juvenile *Buenoa macrotibialis* (Hemiptera: Notonectidae) on the zooplankton of a shallow pond. *Limnology and Oceanography*, *45*, 1006–1012.

Hardy, C. R., & Linder, H. P. (2005). Intraspecific variability and timing in ancestral ecology reconstruction: A test case from the Cape flora. *Systematic Biology*, *54*(2), 299–316.

Hickernell, L. M. (1917). A study of desiccation in the rotifer, *Philodina roseola*, with special reference to cytological changes accompanying desiccation. *The Biological Bulletin*, *32*(6), 343–406.

Hochberg, R., Araújo, T. Q., Walsh, E. J., Mohl, J. E., & Wallace, R. L. (2023). Fine structure of the retrocerebral organ in the rotifer *Trichocerca similis* (Monogononta). *Invertebrate Biology*, *142*(1), e12396.

Houy, S., Croisé, P., Gubar, O., Chasserot-Golaz, S., Tryoen-Tóth, P., Ory, S., & Gasman, S. (2013). Exocytosis and endocytosis in neuroendocrine cells: Inseparable membranes!. *Frontiers in Endocrinology*, *4*, 62255.

Hyman, L. H. (1951). The invertebrates: Acanthocephala, Aschelminthes, and Entoprocta. In E. J. Boell (Ed.), *The pseudocoelomate Bilateria* (pp. vii+–573). McGraw-Hill.

Jørgensen, C., Kørboe, T., Møhlenberg, F., & Riisgård, H. (1984). Ciliary and mucus-net filter feeding, with special reference to fluid mechanical characteristics. *Marine Ecology Progress Series*, *15*(3), 283–292.

Kappner, I., Al-Moghrabi, S., & Richter, C. (2000). Mucus-net feeding by the vermetid gastropod *Dendropoma maxima* in coral reefs. *Marine Ecology Progress Series*, *204*, 309–313.

Kiφrboe, T., & Titelman, J. (1998). Feeding, prey selection and prey encounter mechanisms in the heterotrophic dinoflagellate *Noctiluca scintillans*. *Journal of Plankton Research*, *20*(8), 1615–1636.

Koste, W. (1978). Rotatoria. Die Radertiere Mittel-Europas, 2nd ed. Gebruder Borntraeger, Berlin and Stuttgart. V. 1, text, 673 p.; V. 2, plates, 476.

Meldolesi, J., & Ceccarelli, B. (1981). Exocytosis and membrane recycling. *Philosophical Transactions of the Royal Society of London. B, Biological Sciences*, *296*(1080), 55–65.

Mellman, I., Fuchs, R., & Helenius, A. (1986). Acidification of the endocytic and exocytic pathways. *Annual Review of Biochemistry*, *55*(1), 663–700.

Montgomery, Jr., T. H. (1903). On the morphology of the rotatorian family Floscullariidae. *Proceedings of the Academy of Natural Sciences of Philadelphia*, *55*, 363–395.

Nance, J. M., & Braithwaite, L. F. (1979). The function of mucous secretions in the cushion star *Pteraster tesselatus* Ives. *Journal of Experimental Marine Biology and Ecology*, *40*(3), 259–266.

Nozais, C., Duchêne, J. C., & Bhaud, M. (1997). Control of position in the water column by the larvae of *Poecilochaetus serpens* (Polychaeta): The importance of mucus secretion. *Journal of Experimental Marine Biology and Ecology*, *210*(1), 91–106.

Obertegger, U., & Wallace, R. L. (2023). Trait-based research on Rotifera: The holy grail or just messy. *Water*, *15*(8), 1459.

de Paggi, S. B. J. (2002). Family Asplanchnidae Eckstein, 1883. Rotifera. Vol. 6: Asplanchnidae, Gastropodidae, Lindiidae, Microcodidae, Synchaetidae, Trochosphaeridae and *Filinia*. In H. J. Dumont (Ed.), *Guides to the Identification of the Microinvertebrates of the Continental Waters of the World* (Vol. 18, pp. 1–27). Backhuys.

de Paggi, S. B. J., Wallace, R., Fontaneto, D., & Marinone, M. C. (2020). Phylum Rotifera. In C. Damborenea, D. C. Rogers, & J. H. Thorp (Eds.), *Thorp and Covich's freshwater invertebrates* (pp. 145–200). Academic Press.

Pavelka, M., & Roth, J. (2015). *Functional ultrastructure: Atlas of tissue biology and pathology*. Springer. https://doi.org/10.1007/978-3-7091-1830-6

Petersen, J. K. (2007). Ascidian suspension feeding. *Journal of Experimental Marine Biology and Ecology*, *342*(1), 127–137.

Remane, A. (1933). Rotatoria (4. Lieferung). In H.G. Bronn (Ed.), *H.G. Bronn's Klassen und Ordnungen des Tier-Reichs*. Vierter Band: Vermes. II. Abteilung: Aschelminthen. I. Buch: Rotatorien, Gastrotrichen und Kinorhynchen (pp. 452–576). Akademische Verlagsgesellschaft.

Rutter, G. A., & Tsuboi, T. (2004). Kiss and run exocytosis of dense core secretory vesicles. *Neuroreport*, *15*(1), 79–81.

Shiel, R. J., & Koste, W. (1993). Rotifera from Australia inland waters. IX. Gastropodidae, Synchaetidae, Asplanchnidae (Rotifera: Monogononta). *Transactions of the Royal Society of Australia*, *117*(3), 111–139.

Snell, T. W. (1998). Chemical ecology of rotifers. *Hydrobiologia*, *387*, 267–276.

Sørensen, M. V., & Giribet, G. (2006). A modern approach to rotiferan phylogeny: combining morphological and molecular data. *Molecular Phylogenetics and Evolution*, *40*(2), 585–608.

Sudzuki, M. (1955). Life history of some Japanese Rotifers I. *Science Reports of the Tokyo Daigaku Dai*, *118*, 41–63.

Sudzuki, M. (1957a). Studies on the egg-carrying types in Rotifera. II. Genera *Brachionus* and *Keratella*. *Zoological Magazine, Tokyo*, *66*, 11–20.

Sudzuki, M. (1957b). Studies on the egg-carrying types in Rotifera III. Genus *Anuraeopsis* Japan., engl. summ. *Zoological Magazine, Tokyo*, *66*, 407–415.

Vasilikopoulos, A., Herlyn, H., Fontaneto, D., Wilson, C. G., Nowell, R. W., Flot, J. F., Barraclough, T. G., & Van Doninck, K. (2024). Whole-genome analyses converge to support the Hemirotifera hypothesis within Syndermata (Gnathifera). *Hydrobiologia*, *851*(12), 2795–2826.

Verdugo, P. (2005). Polymer gel phase transition in condensation-decondensation of secretory products. *Advances in Polymer Science*, *110*, 145–156.

Walsh, E. J. (1989). Oviposition behavior of the littoral rotifer *Euchlanis dilatata*. *Hydrobiologia*, *186–187*, 157–161.

Walsh, E. J., Wallace, R. L., & Shiel, R. J. (2005). Toward a better understanding of the phylogeny of the Asplanchnidae (Rotifera). *Hydrobiologia*, *546*, 71–80.

Wierzejski, A. (1893). Rotatoria (wrotki) Galicyi. *Nakładem Akademii Umiejętności*. Sklad Glôwny W Ksiegarnu Spólki Wydawniczej Polskiej

Wurdak, E. S. (1987). Ultrastructure and histochemistry, of the stomach of Asplanchna sieboldi. *Hydrobiologia*, *147*, 361–371.

Wurdak, E. (2017). External morphology of the eggs of Asplanchnopus multiceps (Schrank, 1793) (Rotifera): Solving the 150-year-old case of mistaken identity. *Hydrobiologia*, *796*, 161–168.

Yang, H., & Hochberg, R. (2018a). Ultrastructural and elemental characterization of the extracorporeal tube of the sessile rotifer *Floscularia conifera* (Rotifera: Gnesiotrocha). *Invertebrate Biology*, *137*(4), 319–328.

Yang, H., & Hochberg, R. (2018b). Ultrastructure of the extracorporeal tube and "cement glands" in the sessile rotifer *Limnias melicerta* (Rotifera: Gnesiotrocha). *Zoomorphology*, *137*(1), 1–12.

Yang, H., Hochberg, R., Walsh, E. J., & Wallace, R. L. (2021). Ultrastructure of extracorporeal secretions of four sessile species of Rotifera (Gnesiotrocha), with observations on the chemistry of the gelatinous tube. *Invertebrate Biology*, *140*(2), e12318.

Štrojsová, M., & Vrba, J. (2007). Rotifer digestive enzymes: Direct detection using the ELF technique. *Hydrobiologia*, *593*, 159–165.

SUPPORTING INFORMATION

Additional supporting information can be found online in the Supporting Information section at the end of this article.

How to cite this article: Hochberg, R., Wallace, R. L., Walsh, E. J., & Araújo, T. Q. (2024). Ultrastructure of the extraordinary pedal gland in *Asplanchna* aff. *herricki* (Rotifera: Monogononta). *Journal of Morphology*, *285*, e21765. https://doi.org/10.1002/jmor.21765